Ocean Engineering 151 (2018) 71–81

Contents lists available at ScienceDirect

Ocean Engineering

journal homepage: www.elsevier.com/locate/oceaneng

Numerical simulation for the tip leakage vortex cavitation

Qiang Guo [a,b], Lingjiu Zhou [a,c,*], Zhengwei Wang [d], Meng Liu [a], Huan Cheng [a]

[a] College of Water Resources and Civil Engineering, China Agricultural University, Beijing, China
[b] School of Hydraulic Energy and Power Engineering, Yangzhou University, Yangzhou, China
[c] Beijing Engineering Research Center of Safety and Energy Saving Technology for Water Supply Network System, Beijing, China
[d] Department of Energy and Power Engineering, Tsinghua University, Beijing, China

ARTICLE INFO

Keywords:
Tip leakage vortex
Cavitation
Eddy-viscosity model
Rotation-curvature correction

ABSTRACT

The tip leakage vortex (TLV) cavitation is investigated by a commercial Reynolds averaged Navier-Stokes (RANS) solver. A referenced test on a NACA0009 hydrofoil is used to validate the numerical simulation. Considering the local rotation characteristics of the vortical flow, a rotation-curvature corrected Shear-Stress-Transport model (SST-CC model) is applied to simulate the time-averaged turbulent flow. Compared to the original SST model, the SST-CC model improves the prediction of the velocity in TLV on the measured sections in downstream, and the vorticity and pressure features along the TLV trajectory are analysed numerically. In order to increase the prediction accuracy for the TLV cavitation, the empirical condensation coefficient (F_c) in Zwart's cavitation model is calibrated based on the referenced experiment. By introducing a vortex identification parameter (f^*) related to the strain rate tensor and the vorticity tensor, a relationship between the F_c and f^* is built, and the effects of the rotational motion of the vortex on the cavity are embodied in a modified Zwart's cavitation model. Compared to the conventional Zwart's cavitation model, the modified cavitation model significantly improves the prediction of the TLV cavitation and gets a better agreement with the referenced test on different conditions with various gap widths.

1. Introduction

The rotor tip clearance is inevitable in many axial flow hydraulic machineries, such as the Kaplan and bulb turbines, axial pumps and shrouded propulsors. The tip clearance can result in the leakage flow and the formation of vortices. Among various vortices, the tip leakage vortex (TLV) has the highest total pressure drop and the highest total pressure loss (Xiao et al., 2001), and the resulting vortex cavitation raises much concerns, such as the severe erosion near the blade tip, the performance deterioration, unit vibration and the acoustic noise (Laborde et al., 1997; Avellan, 2004). The cavitating TLV draws much attention for a long time, but this flow is complex and not well understood until recently (Liu et al., 2015; Luo et al., 2016). The confused physics involved in vortex cavitation is that the cavitation is not only induced in vortical structures but is also a source of vorticity (Arndt, 2002). Most of the new advances rely on the application of new experimental techniques and the development of computational tools.

Tan et al. (2015). used a transparent acrylic rotor allowing uninhibited visual access to the cavitation phenomena in an axial waterjet pump. The interactions between the TLV and the cloud cavitation were investigated by high-speed imaging. Particle imaging velocimetry (PIV) is usually used to examine the vortical flows with cavitation suppressed. The rollup process of the TLV was identified by Wu et al. (2011), but multiple interlaced vortical structures in rotor disturbed the TLV and increased the flow variability (Oweis and Ceccio, 2005). An in-depth study on the primary TLV is usually by means of a hydrofoil. For example, Gopalan et al. (2002). measured the velocity and thus vorticity and circulation of TLV in several planes, and Dreyer et al. (2014). adopted the stereo PIV to investigate the 3D flow fields. In these experiments, the cavitation phenomenon is a way of showing the TLV trajectory, but the internal flow test on the cavitation condition is relatively difficult.

The computational fluid dynamics (CFD) is helpful to explore more extensive characteristics of the cavitating vortex. A commercial Reynolds averaged Navier-Stokes (RANS) solver in conjunction with a turbulence model and a cavitation model is generally adopted for engineering practice, but the simulation results usually have a much shorter or smaller cavitation region than the experimental observations for different kinds of vortex cavitation (Decaix et al., 2015a; Wang et al., 2014; Zhou et al., 2017). In order to improve the predictions, most efforts

* Corresponding author. 17 Qinghua Donglu, Beijing 100083, China.
E-mail address: zlj@cau.edu.cn (L. Zhou).

https://doi.org/10.1016/j.oceaneng.2017.12.057
Received 14 January 2017; Received in revised form 27 October 2017; Accepted 24 December 2017

have been done to develop the calculation models. The eddy viscosity turbulence model is a particularly important way to simulate the turbulent flow. Currently, the most prominent model is the k-ω based Shear-Stress-Transport (SST) model (Menter, 1994), which could capture the global features of the TLV in much previous examples (Kato et al., 2011; Decaix et al., 2015b; Guo et al., 2016). Smirnov and Menter (2009) put a rotation-curvature correction (CC) term into the original SST model to form a SST-CC model. It could increase the prediction accuracy for the non-cavitating vortex evolution (Smirnov and Menter, 2009; Arolla and Durbin, 2014), but its application on the cavitating TLV is not clear. The cavitation model is another key factor affecting the prediction of vortex cavitation. In the Eulerian-Eulerian multiphase flow field, the mass transfer models proposed by various authors (such as Kunz et al. (2000), Singhal et al. (2002), Zwart et al. (2004). and so on) have demonstrated their capabilities to reproduce the main features of cavitating flows for decades (Frikha et al., 2009). These cavitation models share the common feature of employing empirical coefficients, which are determined through numerical/experimental results and are adjusted for different geometries and different flow conditions. According to calibrating the coefficient values, a larger resemblance can be observed among most cavitation models. The effects of the coefficient from three models (Kunz et al., 2000; Singhal et al., 2002; Zwart et al., 2004) on the computed results of the cavitating tip vortex in propellers have been analysed (Morgut and Nobile, 2012), and it reveals that further improvement on the simulated cavity extension is needed. In consideration of the cavitation-vortex interactions, Zhao et al. (2016). have built a relationship between the cavitation bubble radius and vortex effects based on the Zwart's cavitation model, and the predictive ability of a new vortex cavitation model has been verified. The above researches have achieved a certain positive effect respectively, but a comprehensive evaluation for the effects of both turbulence model and cavitation model is not enough on the complicated TLV flow and cavitation.

The aim of this study is to evaluate the calculation models for simulating the TLV and its cavitation. A referenced hydrofoil test in the single phase flow and the multiphase flow is used to validate the simulated results. Numerical setups are shown in Section 2. In Section 3, the non-cavitating vortex flow is analysed by the SST-CC turbulence model, whose influence on predicting the cavitating TLV is analysed in Section 4. In the multiphase flow, the empirical coefficient in Zwart's cavitation model is calibrated based on the vortex intensity, and a modified cavitation model is established. Finally, the conclusions are summarized in Section 5.

2. Numerical setups

2.1. Governing equations

A commercial CFD code of ANSYS CFX (ANSYS CFX, 2011) is used in present work with a RANS solver. In the following steady-state equations, the bar is dropped for averaged quantities, except for products of fluctuating quantities.

$$\frac{\partial \rho}{\partial t}+\frac{\partial}{\partial x_j}\left(\rho u_j\right)=0 \tag{1}$$

$$\frac{\partial}{\partial t}\left(\rho u_i\right)+\frac{\partial}{\partial x_j}\left(\rho u_i u_j\right)=-\frac{\partial p}{\partial x_i}+\frac{\partial}{\partial x_j}\left(\mu\frac{\partial u_i}{\partial x_j}-\rho\overline{u_i'u_j'}\right)+S_M \tag{2}$$

where u_i ($i=u, v, w$) is the velocity, x_i ($i=x, y, z$) is the position, t is the time, p is the pressure, μ is the dynamic viscosity, S_M is the external momentum source term. The Reynolds stresses $\rho\overline{u_i'u_j'}$ can be modified by a turbulence model.

For the multiphase flow, the homogeneous (one-fluid) model allows some simplifications with an assumption that the transported quantities are the same for all phases, except for the volume fraction α. The ρ is defined as the density of mixture with the following definition:

$$\rho=\alpha_v\rho_v+\alpha_l\rho_l \tag{3}$$

where the subscripts v and l represent the vapor and liquid phases respectively.

2.2. Computational domain and mesh validation

Referring to Dreyer et al.'s experiment (Dreyer, 2015), a NACA0009 hydrofoil had the truncated chord (c) of 100 mm and its maximum thickness (h) was 9.9 mm, which was tested in a water tunnel with a 150 mm wide cross section and 750 mm length. There was a gap between the foil tip and the tunnel lateral wall, and the cavity extension is different with various gap widths. A non-dimensional parameter τ was defined as the ratio of the absolute gap width and the foil thickness, and two typical conditions with $\tau=0.2$ and $\tau=1$ are discussed here with different cavity extension. The computational domain with boundary conditions is shown in Fig. 1. The inlet which is located in the upstream with about $2c$ distance to the foil leading edge has a velocity of $V_{in}=10$ m/s with low turbulence intensity (below 1%), the outlet has a static pressure to maintain the inlet pressure p_{in} near 1 bar, no slip walls are at the other boundaries, and the foil incidence angle is 10°.

A structured hexahedral mesh is generated in the computational domain with Fig. 2 showing the local mesh near the foil tip. Based on the Richardson extrapolation method, which is currently the most reliable method available for the prediction of numerical uncertainty, a Grid Convergence Index (GCI^{21}_{fine}) is used to validate the mesh resolution (Celik et al., 2008). The detailed process for mesh validation has been finished in our previous work (Guo et al., 2016). The pressure coefficient $C_P=(p\text{-}p_{in})/(0.5\rho V_{in}^2)$ in the TLV core is chosen as a key variable. When the convergence index GCI^{21}_{fine} for C_P is within 5%, the total number of mesh cells about 4.4 million is used. The averaged $y+$ is 20 and 60 for the maximum on the foil surface and both sides of the gap. In the simulation, the high resolution scheme is used for the advection scheme and convergence is specified as RMS residuals of 10^{-5}.

3. Simulation of the non-cavitating TLV flow

3.1. Rotation-curvature correction for the eddy viscosity model

The gradient diffusion hypothesis is frequently used in numerical simulations of turbulent flows involving transport equations. The eddy viscosity turbulence models use this hypothesis to relate the Reynolds stresses to the mean velocity gradients and the eddy viscosity (μ_t). The μ_t can be linked to the turbulence kinetic energy (k) and turbulent frequency (ω) via this relation:

$$\mu_t=\rho\frac{k}{\omega} \tag{4}$$

and then many k-ω models are formed. The k-ω SST (shear stress transport) model of Menter (1994) accounts for the transport of the turbulent shear stress and gives highly accurate predictions of the onset and the amount of flow separation under adverse pressure gradients.

One of the weaknesses of eddy viscosity models is that they are not

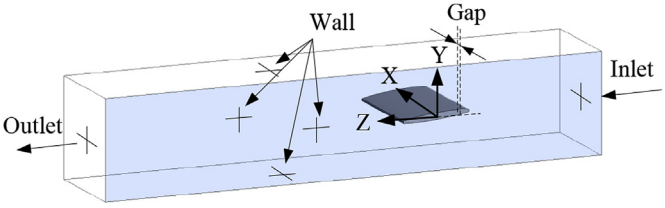

Fig. 1. Computational domain and boundary conditions.